Journal of Thermal Analysis and Calorimetry, Vol. 96 (2009) 2, 587–592

EFFECTS OF NANOCLAY ON THE THERMAL AND RHEOLOGICAL PROPERTIES OF A VARTM (VACUUM ASSISTED RESIN TRANSFER MOLDING) EPOXY RESIN

Roberta Peila[1*], *J. C. Seferis*[2], *T. Karaki*[3] *and G. Parker*[4]

[1]Polytechnic of Turin-Chemical Engineering Department, C.so Duca degli Abruzzi 24, Turin, Italy
[2]Glocal Network Corporation, Seattle WA 98121, USA
[3]Toray Industries Inc., Japan
[4]The Boeing Company, Seattle-WA 98124, USA

Three types of commercially available organophilic Montmorillonite (Cloisite 30B, 25A and 15A) were used to prepare VARTM epoxy resin nanocomposites in order to study the effect of the nanoclay organophilic modification on the epoxy matrix. The morphology of the dispersions was investigated through XRD and TEM analyses. The thermal stability of the nanocomposites was studied by means of HI-RES TG measurements and the influence of the nanoclay on the viscosity of the resin was investigated through rheological measurements. It was found that the nanoclay modification had no significant influence on the dispersion and on the thermal properties of the nanocomposites. Areas of exfoliated and intercalated morphology were observed. The viscosity of the resin furthermore did not exceed the critical value of the infusion process.

Keywords: *epoxy resin, nanocomposites, organo-montmorillonites, thermal stability, VARTM, viscosity*

Introduction

The improvements in process control of liquid infusion processes that offer void free parts, dimensional reproducibility and surface finish of composites have sparked renewed interest in these techniques. They are very valuable due to their great cost savings, particularly when compared to autoclave-cured techniques of composites manufacturing. Among them Vacuum Assisted Resin Transfer Molding (VARTM) is considered the most cost-effective manufacturing method, allowing cost saving of up to 75% with respect to standard processes. VARTM is a very simple process because only a one-piece mold and a vacuum bag are required with no mechanical pressure during the infusion of the resin. A preform is placed between the mold and a vacuum bag and a vacuum pump creates the vacuum inside the system. The pressure differential causes the resin to flow through the preform. The flow of the resin in the preform is described by Darcy's law:

$$u = \frac{k}{\mu} \nabla P$$

where u is the volume averaged velocity vector of the resin, μ is the Newtonian viscosity of fluid, P is the pressure gradient vector, and k is the permeability tensor of the porous medium. The ∇P is dictated by the pump and the preform permeability is responsible for the fiber wet-out. To allow the resin and the cross-linking agent to form the network structure, the sample is placed in an oven where the curing reaction takes place. After it is completed the composite is removed from the mold. Sometimes the heterogeneity and the non-uniformity of the preforms can cause dry spots and voids in the final composite. Numerical models have been studied to control and overcome this problem [1–6]. Most of the time the preform remains the same so the only parameter that regulates the flow behavior is the viscosity of the resin. Constraints fix the maximum infusible value at 300/500 cP, since increasing the resin viscosity reduces its capability to flow and to be homogeneously distributed through the sample [2]. The limitations in resin viscosity coupled with the inferior mechanical properties of the final composites, when compared to those that were autoclave cured, necessitate studies on the toughening of VARTM compounds. Seferis and coworkers have tried to strengthen VARTM samples by spraying tackifiers of preformed rubber particles on woven carbon fibers showing a good increase in interlaminar fracture toughness [3, 7, 8]. In addition work is under way on the reinforcement of the composite matrix with nanoparticles [9–11].

The emphasis on the experimentation involving nanofiller is mostly due to the nanofiller unique phase

* Author for correspondence: roberta.peila@polito.it

1388–6150/$20.00

Akadémiai Kiadó, Budapest, Hungary
Springer, Dordrecht, The Netherlands

morphology and interfacial properties that improve the performance of composites. Nanoclays are particularly explored as a matrix toughening component for their high aspect-ratio, plate morphology, natural availability and low cost. They are known to enhance properties such as stiffness, modulus and toughness, barrier and flame retardance [12–14]. Some restrictions in their use however arise from their agglomerated tactoidal structure. This structure and the resulting high cohesive energy cause problems in the dispersion at a nano-scale length in the polymer matrix. Nanoclay with surface ion exchange functionalization are commercially available and allow a better interaction with the matrix by lowering the surface energy and the hydrophilicity of the clay. The morphology of the clay in the polymer matrix as well plays an important role on the final properties of the composite materials. In the exfoliated states the nanoclay are known to enhance the mechanical, barrier and flame resistance properties of the composites even at relatively low concentrations. It is the polymerization of the resin molecules that starts the exfoliation mechanism: the resin molecules penetrate into the silicate layers due to the attraction of the clay high surface energy and swell them until the system reaches a thermodynamic equilibrium. During this reaction the polarity of the resin is decreased allowing more resin molecules to penetrate into the layers promoting an exfoliated structure. The extent of intercalation and exfoliation depends on the clay concentration, type of clay, type of resin, curing agents and curing conditions [15–27].

As stated above in VARTM processing one of the main factors that have to be controlled is the viscosity of the resin. It is known that the addition of fillers causes an increase in viscosity, due to the high surface area and aspect ratio of the nanoclay that intensify the friction in the interaction with the resin [2]. In this work we studied the interaction between an epoxy resin currently used in VARTM processes and quaternary ammonium salt modified nanoclay. The thermal properties of the neat resin and the nanocomposites were studied as well as the morphology of the nanoclay in the epoxy matrix. In addition analysis on the viscosity of the prepared samples were performed by rheological measurements.

Experimental

Materials and experimental procedures

Resin and nanocomposites preparation

The VARTM resin and the cross-linking agent were provided by Toray Industries, Inc, Japan. The nanoclay used as reinforcement were commercially available from Southern Clay Products, USA. Three different types of quaternary ammonium salt modified nanoclay were analyzed: Cloisite 30B modified with bis-2-hydroxyethyl methyl tallow quaternary ammonium; 25A modified with dimethyl 2-ethylhexyl hydrogenated tallow quaternary ammonium and 15A modified with dimethyl dehydrogenated tallow quaternary ammonium.

The resin systems were prepared by adding 2 and 5 parts per hundred (phr) of each nanoclay to the resin previously heated at 40°C for 10 min. After the addition of the nanoclay the system was mixed for 30 min with a Dispersmat mixer at 1000 rpm to ensure a good dispersion of nanoclay. A stoichiometric amount of curing agent was added to the system for the curing of the resin. The nanocomposites were cured in an oven at 120°C for 2 h.

Methods

Morphology of the nanoclay

A Philips 1820 X-Ray Diffractometer with an acceleration voltage of 40 kV, coupled with a 20 mA current, was used to examine the morphology of the nanoclay into the epoxy matrix. Measurements were carried out at 2° min^{-1} rate in a 3 to 20° 2θ range.

TEM analysis were performed in order to verify the XRD results. The samples were cut using a 3 mm disc cutter with silicon carbide powder (grit 600) and then thinned and polished using PK/100 Silicon Carbide (1200 abrasive grade) discs. They were eventually thinned with a Gatan dimple grinder before being placed in a Gatan Ion Mill (model 600) for 6 h. The micrographs were obtained with an EM 420T TEM 140 microscope using an acceleration voltage of 120 kV.

Rheological measurements

A 2% strain controlled test of 1 Hz frequency, was carried out on pre-cured nanocomposites using a Rheometric Dynamic Analyzer DMA-RMS 800 with a temperature ramp of 2°C min^{-1} from 30 to 120°C. The experiments were conducted using parallel plate geometry with a 25 mm disc size and 1 mm gap width.

Before the analysis the hardener was added to the mixture of the resin and nanoclay and manually mixed for 2 min.

An isothermal hold at 6°C for 1 h was conducted using an oscillatory rheometer RD/2 with parallel plate geometry with a 25 mm disc size.

Thermal properties

A HI-RES TGA 2950 thermogravimetric analyzer was used to perform the thermal analysis on the samples. The analyses were carried out under nitrogen at

a flow rate of 105/115 cm^3 min^{-1} with an initial temperature ramp of 30°C min^{-1}, resolution 3, and sensitivity 4, from room temperature to 1000°C.

The mass of the samples analyzed was 10/12 mg. The mass changes as well as the derivatives of the mass changes were registered.

Results and discussions

Morphology of the nanoclay

Figures 1, 2 and 3 represent the X-ray diffraction patterns of the nanocomposites prepared compared to the neat nanoclay. In Fig. 1 the wide peak at 2θ=4.8° is characteristic of the neat 25A nanoclay, corresponding to a *d*-spacing of 18.6 Å in correlation to the Bragg equation. The absence of significative peaks, in the lower 2θ range in the nanocomposites diffractograms, indicates a possibly exfoliated structure due to the penetration of the epoxy resin into the clay layers. This penetration is favored by the ion exchange functionalization of montmorillonite nanoclay with organic cations that makes the hydrophilic nanoclay hydrophobic and cause them to be more compatible with the epoxy matrix. In Fig. 2 the *d*-spacing of the 30B neat nanoclay is 18.0 Å and the main reflection peak is at 2θ=4.9°. In Fig. 3 the absence of the main peak of the neat nanoclay is due to some limitations of the instrument that didn't allow detecting the region below 2θ=3°. The broad peak that starts at 2θ=12° is characteristic of the epoxy resin. The results obtained for the nanocomposites suggested that the different types of nanoclay exhibited the same behavior from a morphological standpoint. The concentration of the nanoclays as well did not lead to a different performance.

In order to confirm these results a direct observation with a transmission electron microscope was

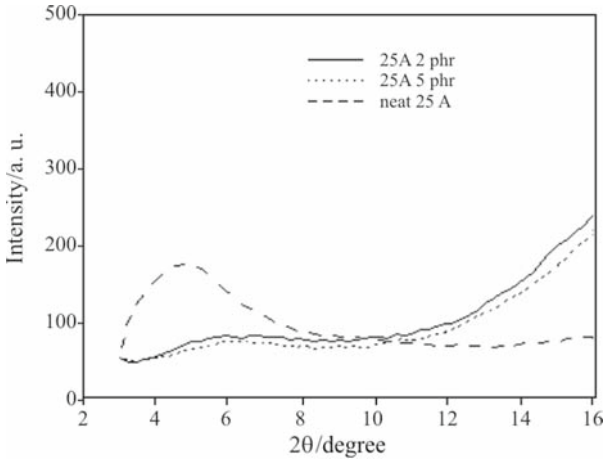

Fig. 1 XRD diffraction patterns of the 25A/epoxy resin nanocomposites

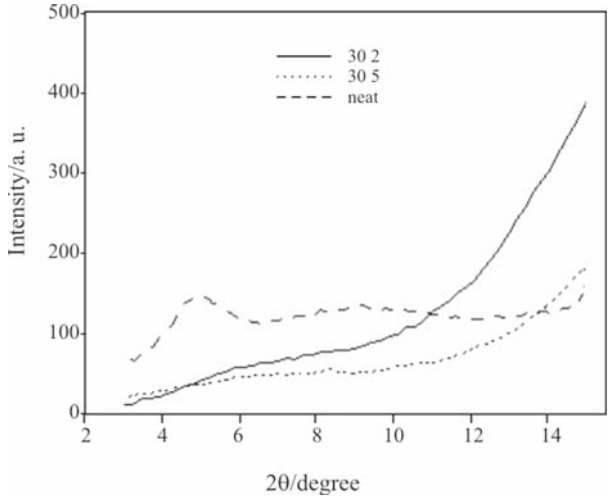

Fig. 2 XRD diffraction patterns of the 30B/epoxy resin nanocomposites

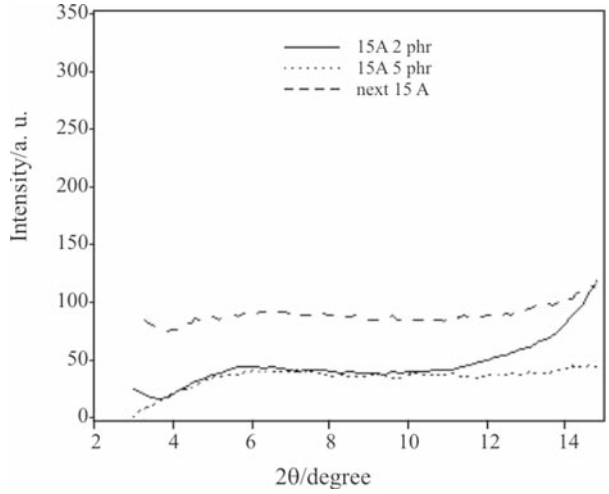

Fig. 3 XRD diffraction patterns of the 15A/epoxy resin nanocomposites

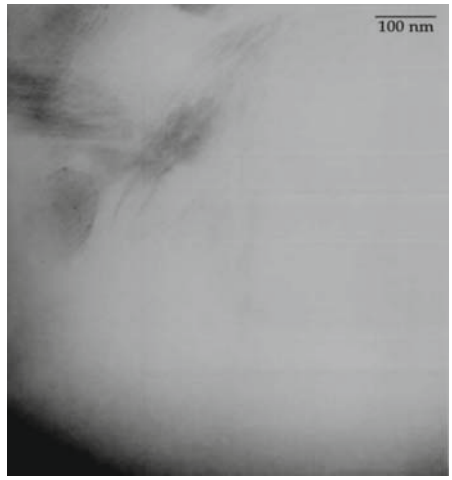

Fig. 4 TEM of the 30B/epoxy nanocomposite (5 phr)

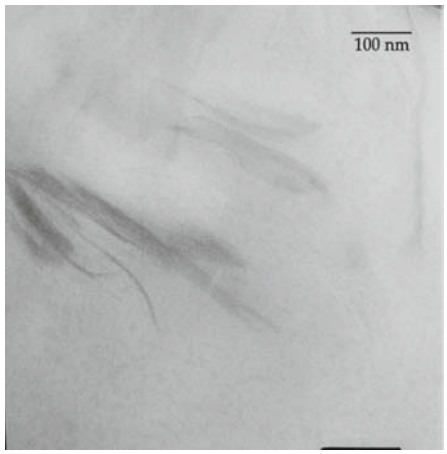

Fig. 5 TEM of the 15A/epoxy nanocomposite (5 phr)

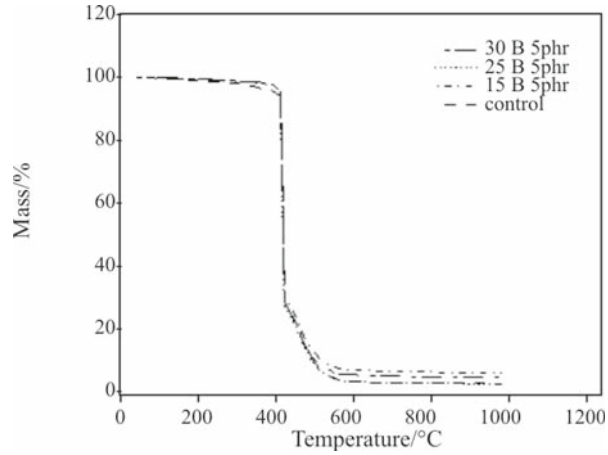

Fig. 6 Mass loss for the 5 phr nanocomposites

made on same nanocomposites. TEM pictures in Figs 4 and 5 show some regions of exfoliated morphology and others with nanoclay still in their respective tactoidal and intercalated structures.

Thermal properties

The curves of Figs 6 and 7 show the mass loss and the derivative of the mass loss of the samples containing 5 phr of the different types of nanoclay. The curves of each sample showed that the degradation consisted of two steps and that the maximum degradation rate occurred at almost the same temperatures. The difference of 3 to 4°C among the degradation temperatures, reported in Table 1, indeed, is not significant. The temperature of initial degradation (T_i) was measured as well. In literature it is cited that this temperature can be used to estimate the thermal stability of the material analyzed [14]. It is the temperature at which a 5% of mass loss occurs. In Table 1 these values are reported for the 5 phr nanoclay/epoxy resin nanocomposites. The measured temperatures demonstrated that the T_i of the nanocomposites increased of 12 to 14°C. This increase can be attributed to the exfoliated and intercalated morphology of the nanoclay into the resin matrix, as shown by the TEM and XRD results. The type of nanoclay, on the other hand, didn't affect the thermal behavior.

The 2 phr nanocomposites did not differ substantially from the control resin therefore the results were omitted.

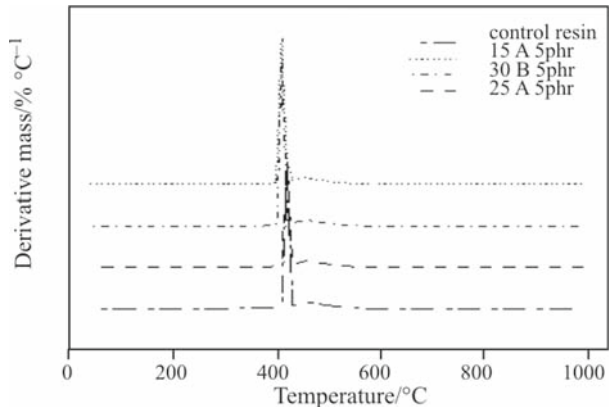

Fig. 7 Derivative of the mass loss for the 5 phr nanocomposites

Rheological analysis

Figures 8 to 10 report the viscosity values of the resin with the temperature. It can be seen that the addition of the nanoclay caused a general raise in the viscosity of the samples. The sharper increase of the nanocomposites curves, furthermore, evidenced an accelerating mechanism of the curing process. This is attributed to the presence of the onium ions of the modified nanoclay that initiated the polymerization of the epoxy resin [16]. In Fig. 10 the higher slope of the curve containing 2 phr 15A nanoclay is probably due to a better dispersion of the nanoclay into the matrix that advanced the curing mechanism.

Table 1 Maximum degradation temperatures and temperatures of initial degradation for the 5 phr nanocomposites

Sample	Concentration/ phr	Maximum degradation temperature/°C	Temperature of initial degradation/°C
Control resin	0	415	403
30B/epoxy resin	5	414	417
25A/epoxy resin	5	413	414
15A/epoxy resin	5	413	415

In Table 2 the lowest viscosity values and their related temperatures are reported. These temperatures are significant for the infusion process that is facilitated at low viscosities.

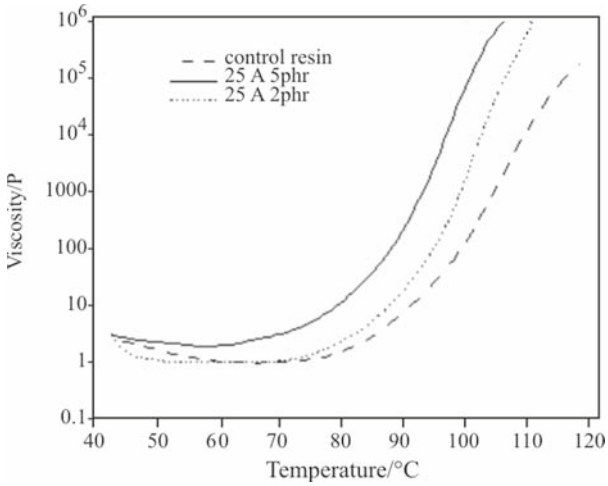

Fig. 8 Viscosity of 25A/epoxy nanocomposites

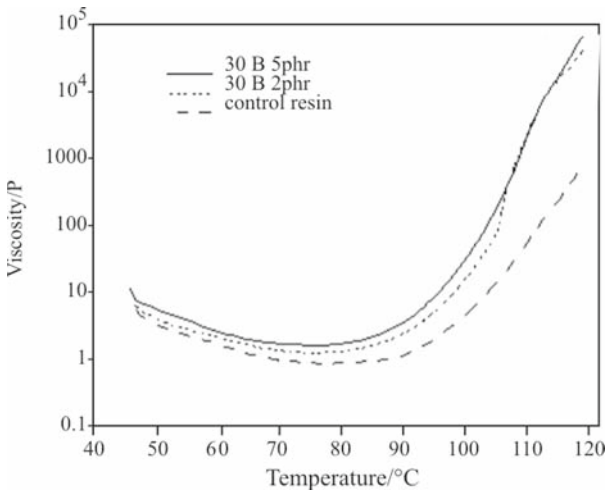

Fig. 9 Viscosity of 30B/epoxy nanocomposites

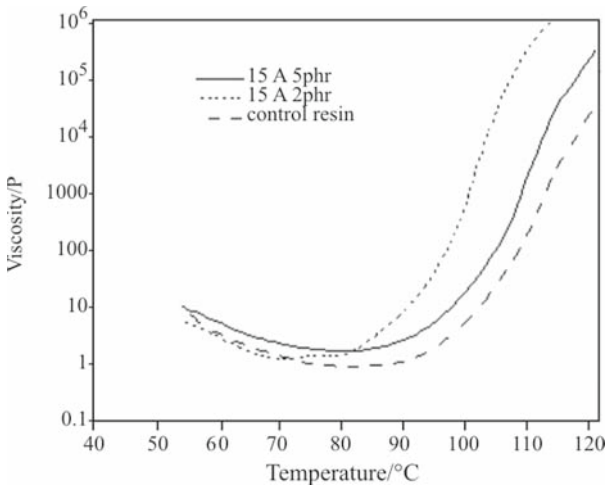

Fig. 10 Viscosity of 15A/epoxy nanocomposites

Table 2 Lowest viscosity values of the nanocomposites

Sample	Concent./ phr	Temp./ °C	Viscosity/ P
Control resin	0	56	0.9
30B/epoxy resin	2	64	1.3
25A/epoxy resin	2	57	0.9
15A/epoxy resin	2	64	1.4
30B/epoxy resin	5	63	1.7
25A/epoxy resin	5	56	1.7
15A/epoxy resin	5	64	1.7

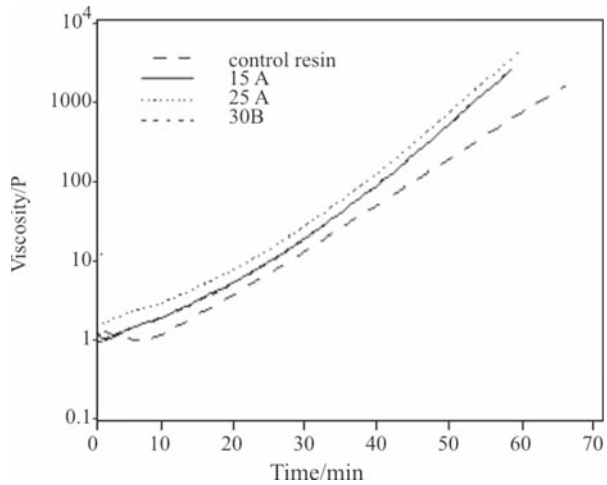

Fig. 11 5 phr nanocomposites isothermal hold at 60°C for 1 h

Literature regarding the infusion process proved that the viscosity of the resin needs to remain below 300 cP not to inhibit the infusion [2]. Figure 11 reports the variations of the viscosity during an isothermal hold for 1 h. It was chosen a temperature of 60°C as an average among the values reported in Table 2. The isothermal hold displayed that after 10 min the viscosity of the nanocomposites increased dramatically, signifying that the infusion process can be affected at this temperature. In our experiments we used a temperature of 40°C as a compromise.

Conclusions

The effects of the addition of different types of nanoclay on the properties of epoxy nanocomposites were investigated. The results showed that there was no significant difference in the type of nanoclay used. The nanoclay were dispersed into the matrix with areas of exfoliated and intercalated morphology. From a thermal standpoint the samples containing 5 phr nanoclay resulted in a better thermal stability in terms of temperatures of initial degradation. The viscosity of the nanocomposites, during the dynamic rampe, stayed below the value of 300 cP signifying that the

infusion process should not be affected. Future work should investigate more deeply the role of the time dependent viscosity at different temperatures in regards to direct applications in infusion processes.

References

1 E. N. Gilbert, B. S. Hayes and J. C. Seferis, 33rd Int. SAMPE Tech. Conf., Seattle, WA, November, 33 (2001) 1368.
2 F. J. Chase, J. Allison, C. Chen and J. Borges, SAMPE Symp. and Exhib., Long Beach, CA, May 16–20, (2004) 441.
3 B. S. Hayes, E.N Gilbert, J. C. Seferis, R. Moulton and D. Dixon, 32nd SAMPE Tech Conf, Boston, MA, November 5–9, 32 (2000) 294.
4 J. Dai, D. Pellaton and H. T. Hahn, Polym. Comp., 2 (2003) 672.
5 R. J. Johnson and R. Pitchumani, Compos. Sci. Technol., 63 (2003) 2201.
6 R. Mathur, D. Heider, C. Hoffmann, J. R. Gillespie, S. G. Advani and B. K. Fink, Polym. Comp., 22 (2001) 477.
7 E. Depase, B. S. Hayes and J. C. Seferis, Soc. Adv. Mat. Proc. Eng. (SAMPE) Tech. Conf., Seattle, WA, November 4–8, 33 (2001) 1379.
8 E. P. M. Williams and J. C. Seferis, Proc. Soc. Adv. Mat. Proc. Eng. (SAMPE 2003) Symp. Exhib., Long Beach, CA, May 11–15, (2003) 1683.
9 J. P. Killgore, S. S. Sangari, T. Jensen and J. C. Seferis, Soc. Plast. Eng. (SPE) 2005 Ann. Tech. Conf. (ANTEC), Boston, Massachusett, May 1–5 (2005).
10 T. Karaki, S. S. Sangari and J. C. Seferis, Soc. Plast. Eng. (SPE) 2005 Ann. Tech. Conf. (ANTEC), Boston, Massachusetts, May 1–5 (2005).
11 J. P. Killgore, T. Jensen, R. Peila, S. S. Sangari and J. C. Seferis, Soc. Adv. Mat. Proc. Eng. Soc. Adv. Mat. Proc. Eng. (SAMPE) 2004 Symp. Exhib., San Diego, CA, November 15–18 (2004).
12 T. J. Pinnavi and G. W. Beall, Polym. Clay Nanocomp., 7 (2000) 127.
13 S. Peeterbroeck, M. Alexander J. B. Nagy, C. Pirlat, A. Fonseca, N. Moreau, G. Philippin, J. Delhalle, Z. Mekhalif, F. Sporken, G. Beyer and P. Dubois, Compos. Sci. Techol., 64 (2004) 2317.
14 G. Aijuan and L. Guozheng, Polym. Degrad. Stab., 80 (2003) 383.
15 F. Xia-An and O. Syed, Polym. Eng. Sci., 44 (2004) 345.
16 X. Kornmann, H. Lindberg and L. A. Berglund, Polymer, 42 (2001) 4493.
17 O. Becker, Y. B. Cheng, R. J. Varley and G. P. Simon, Macrom., 36 (2003) 1616.
18 M. T. Ton-That, T. D. Ngo, P. Ding, G. Fang, K. C. Cole and S. V. Hoa, Polym. Eng. Sci., 44 (2004) 1132.
19 O. Becker, G. P. Simon and K. Dusek, J. Therm. Anal. Cal., 179 (2005) 29.
20 W. Qi, S. Chunfang and L. Weiwer, J. Appl. Polym. Sci., 90 (2003) 511.
21 M. Jun, Y. Zhong-Zhen, Z. Qing-Xin, X. Xiao-Lin, M. Yiu-Wing and L. Ian, Chem. Mater., 16 (2004) 757.
22 Z. Kailiang, W. Lixin, W. Fang, W. Guangjian and L. Zuobang, J. App. Polym. Sci., 91 (2004) 2649.
23 I. M. Daniel, H. Miyagawa, E. E. Gdoutos and J. J. Luo, J. Therm. Anal. Cal., 43 (2003) 348.
24 P. C. LeBaron, Z. Wang and T. J. Pinnavia, Appl. Clay. Sci., 15 (1999)11.
25 J. Park and S. C. Jana, Macromol., 36 (2003) 8391.
26 G. Janowska, T. Mikołajczyk and M. Olejnik, J. Therm. Anal. Cal., 92 (2008) 495.
27 F. Román, S. Montserrat and J. M. Hutchinson, J. Therm. Anal. Cal., 87 (2007) 113.

Received: June 20, 2008
Accepted: July 17, 2008
Online First: November 11, 2008

DOI: 10.1007/s10973-008-9343-1